Rajshahi University journal of science and engineering
Vol. 46-53 (2018-2025), pp 69-82
DOI: https://doi.org/10.64102/rujse.0766

ISSN 2309-0952 (Print)
ISSN 2408-8803 (Online)

Analytical Solutions and Qualitative Analysis to the Generalized Nonlinear Fractional Schrödinger Model using the Extended Riccati Equation Method

Saikh Shahjahan Miah [1*], Md. Al Amin[2], Md. Abul Kalam Azad[3], Kamruzzaman Khan[4]

Abstract

The generalized nonlinear Schrödinger equation (GNLSE) has been studied upon the standard nonlinear Schrödinger equation (NLSE) to model how complex wave envelopes change in nonlinear and dispersive environments. There are many applications of the model in the areas like nonlinear optics, plasma dynamics, Bose-Einstein condensates, and surface wave studies. In this investigation, we study exact soliton solutions for the space-time fractional GNLSE using a traveling wave transformation. We apply the extended Riccati equation approach (EREA) to find the analytical solutions like rational, trigonometric, and hyperbolic. Our obtained solutions represents periodic and general solitons. Moreover, we study the bifurcation, chaotic, and sensitivity analysis of the GNLSE.

***Keywords**:* Fractional generalized nonlinear Schrödinger model; Extended Riccati equation approach; Analytical solution; Qualitative analysis.

1. **Introduction**

Nonlinear evolution equations (NLEEs) have seen significant development. The models are extensively utilized to study complex physical phenomena across a range of scientific fields (Wang and Gao, 2023), (Kawser et al., 2024). The exploration of soliton solutions (Amin et al., 2025a) provides core study into the nonlinear dynamics in natural systems. The applications solitons span from optical fiber communication networks (Amin et al., 2025b) and plasma physics to Bose-Einstein condensates, shallow water wave theory, and fluid dynamics. The presence of solitons in integrable systems is notable because of its underlying mathematical structure (Liu et al., 2018). Solitons can be modulated in terms of amplitude, phase, or frequency. The solitons are used for encoding and transmitting data over long distances with high reliability. Various types of analytical methods have been developed to find solutions to NLEEs for instances the first integral method (Bekir and Unsal, 2012), exp-function method (Bekir and Boz, 2008), homotopy analysis (Inc, 2008), the (G′/G)(G′/G)-expansion method (Kaplan et al., 2016), unified algebraic and auxiliary equation techniques (Kilic and Inc, 2016), and the modified simple equation approach (Arnous et al., 2017).

---

[1] Department of Mathmatics, Mawlana Bhashani Science and Technology University, Tangail 1902, Bangladesh; Email: skhshahjahan@gmail.com * Corresponding Author
[2] Department of Mathematics, Hajee Mohammad Danesh Science and Technology University, Dinajpur, Bangladesh; Email: alaminhstu18@gmail.com
[3] Professor, Department of Applied Mathematics, University of Rajshahi, Rajshahi 6205, Bangladesh; Email: azad267@gmail.com
[4] Department of Mathematics, Pabna University of Science and Technology, Pabna 6600, Bangladesh; Email: k.khanru@gmail.com

Recently, fractional differential equations have gained prominence for their ability to model complex systems using fewer parameters to study dynamics, stability, and chaotic behavior (Tripathy and Sahoo, 2023) of the models. Numerous definitions of fractional derivatives have been studied like the Riemann-Liouville (R-L) (Lioville, 1832), Grünwald-Letnikov (Grünwald, 1867), (Letnikov, 1868), Caputo (Caputo 1967), modified Riemann-Liouville (mR-L) (Jumarie, 2006), and the conformable derivative (Khalil et al., 2014). Among these, the Caputo, mR-L, and conformable derivatives are widely used. However, these concepts have some limitations like the R-L derivative does not vanish for constant functions, the conformable derivative behaves predictably only within limited domains, and the Caputo derivative requires highly smooth functions to handle. The beta fractional derivative, used to remove the drawbacks, proposed by Atangana in 2016 (Atangana, 2016) offers a more flexible and comprehensive framework. Due to the capacity of this derivative to overcome some of the inherent limitations of previous formulations the derivative has been increasingly adopted in fractional modeling. Fractional Sawada-Kotera differential model has been studied (Shahjahan et al. 2025a) to investigate soliton solutions using extended modified auxiliary equation mapping method. Using the beta derivative, the same approach has been implemented on Yu Toda Sasa Fukuyama evolution model (Shahjahan et al. 2025b) and effective solitary solutions have been determined that have a wide range of applications on mathematical physics and engineering.

Definition: If $r \in \mathbb{R}$ and a function $f(x): [r, \infty) \to \mathbb{R}$, then the beta derivative of $f(x)$ is represented by ${}_0^A D_x^\sigma f(x)$ and defined as (Atangana, 2016):

$$
{}_0^A D_x^\sigma f(x) = \begin{cases} \lim\limits_{\delta \to 0} \dfrac{f\left(x + \delta \left(x + \dfrac{1}{\Gamma(\sigma)}\right)^{1-\sigma}\right) - f(x)}{\delta}, & \forall\, x \geq 0, 0 < \sigma \leq 1 \\ f(x), & \forall\; x \geq 0, \sigma = 0\,, \end{cases}
$$

here σ is the order of the derivative and $\Gamma(\sigma) = \int_0^\infty e^{-x}\, x^{\sigma-1} dx$ is the gamma-function. Then f is said to be β −differentiable provided the above limit exists.

The higher-order nonlinear GNLSE (Lu et al., 2019) with space time beta fractional derivative which has the form:

$$
i(D_t^\sigma q + D_{xxx}^{3\sigma} q) + |q|^2(a v_1 q + i v_2 D_x^\sigma) + i v_3 q(|q|^2)_x = 0, 0 < \sigma \leq 1, \qquad (1.1)
$$

here the function $q = q(x,t)$, is complex, denotes the slowly varying envelope of the electric field, and a_j $(j = 1 \dots 5)$ are nonzero parameters (real) corresponding to various physical effects like self-phase modulation, third order dispersion, group velocity dispersion, self-steeping and the self-frequency shift because of the stimulated Raman scattering. Using planar dynamical theory, the complex dynamical feature and optical solitons (Khan et al., 2023) of the GNLSE have been explored using the complete discriminant system method. Optical soliton solutions of the GNLSE based on self-frequency-shift and kerr-nonlinearity-terms have been found (Ahmad et al., 2023) by implementing the modified tanh expansion approach corresponding to new Riccati solutions. Beside these, the EREA is widely acknowledged for its strength and reliability in conducting analytical investigations. In this research, the method is further implemented to extract a broad spectrum of optical soliton and soliton-like solutions for fractional GNLSE. Moreover, the EREA contributes to a deeper realizing of nonlinear mathematical equations with real-world relevance. Based on current available data, the application of EREA to the GNLSE involving the beta derivative has not yet been explored, despite the method's considerable impact on fractional versions of GNLSE. These motivate us to set the aims of this work to derive both standard and generalized stable soliton solutions for the specified nonlinear fractional equation using the EREA. Our study yields rational, hyperbolic, and trigonometric solution forms those have distinct physical behaviors such as general and periodic solitons. Graphical illustrations of the solutions and qualitative analyses are included to highlight the physical characteristics of these solutions and the model.

We have organized this paper as follows: in Section 2, we outline the methodology. In Section 3, we have studied a comprehensive mathematical analysis of the equation. In section 4, we have focused on the graphical visualization of the obtained solutions. In section 5, we have represented the bifurcation analysis. In section 6, we have discussed the chaotic and the sensitivity analyses. In section 7, we have summarized the key conclusions of the study.

2. The Methodology: Extended Riccati Equation

Let us consider the following fractional NLEE

$$\Xi(\mathrm{q}, \mathrm{M}_t^{\sigma}\mathrm{q}, \mathrm{M}_x^{\sigma}\mathrm{q}, \mathrm{M}_{tt}^{2\sigma}\mathrm{q}, \mathrm{M}_{xx}^{2\sigma}\mathrm{q}, \mathrm{M}_t^{\sigma}\mathrm{q}\mathrm{M}_x^{\sigma}\mathrm{q}, \dots) = 0,\ 0 < \sigma \leq 1, \quad (2.1)$$

where Ξ expresses a polynomial in function q and its distinct fractional derivatives. The following transformation

$$q(x,t) = U(\Omega) \text{ and } \Omega = \frac{a}{\sigma}\left(x + \frac{1}{\Gamma\sigma}\right)^{\sigma} + \frac{b}{\sigma}\left(t + \frac{1}{\Gamma\sigma}\right)^{\sigma}, \quad (2.2)$$

alters Eq. (2.1) to an ODE due to Ω:

$$\mathrm{F}(U, U', U'', U''', \dots\dots\dots) = 0. \quad (2.3)$$

We consider the assumption as the integrating constant is zero against the Eq. (2.3). Since the soliton solutions do not contain arbitrary constants, our considered simplification is justified. Then we eliminate these constants and concentrate on extracting the soliton structure.

Let us consider that the solution to Eq. (2.1) takes the form:

$$U(\Omega) = \frac{\iota_0 + \sum_{i=1}^{n}(\iota_i\phi^i(\Omega) + \varepsilon_i\phi^{-i}(\Omega))}{\kappa_0 + \sum_{i=1}^{n}(\kappa_i\phi^i(\Omega) + \tau_i\phi^{-i}(\Omega))}, \quad (2.4)$$

where $i = 1,2,3,\dots,n$, and the parameters ι_i, ε_i, κ_i and τ_i are constants to be determined. The value of n is obtained using the homogeneous balance method. Additionally, the function $\phi = \phi(\Omega)$ is assumed to satisfy the Riccati differential equation:

$$\phi'(\Omega) = \mu + \lambda\phi(\Omega) + \nu\phi^2(\Omega). \quad (2.5)$$

The exact solutions of the above equation have been determined by Zhu (2008).

By substituting Eq. (2.2) and Eq. (2.3) into Eq. (2.1), a polynomial in terms of ϕ is molded. To find the parameters in Eq. (2.2) as well as in Eq. (2.3), the algebraic equations are solved by taking each coefficient of the polynomial equal to zero. After identifying the parameter values according to this process, solutions for Eq. (2.2) can be determined using the obtained values and the solutions founded by Eq. (2.3).

3. Application of EREA to the GNLSE

We start by introducing a particular transformation of the variable (wave) Ω, defined as follows:

$$q(x,t) = U(\Omega) \text{ and } \Omega = \frac{a}{\sigma}\left(x + \frac{1}{\Gamma\sigma}\right)^{\sigma} + \frac{b}{\sigma}\left(t + \frac{1}{\Gamma\sigma}\right)^{\sigma}, \tag{3.1}$$

where a and b are wave number and wave velocity respectively. This change of variables enables the wave equation to be expressed in terms of the new variable Ω, with U now considered a function of Ω. By inserting the transformation into the Eq. (1.1), we obtain the following expression:

$$i(U_{\Omega} + U_{\Omega\Omega\Omega}) + |U|^2(\nu_1 U + i\nu_2 U_{\Omega}) + i\nu_3 U|U|^2{}_{\Omega} = 0, \tag{3.2}$$

where, U denotes a complex-valued function, and its subscripts indicate differentiation with respect to Ω. To facilitate further simplification, we apply the transformation below to the function $U(\Omega)$:

$$U(\Omega) = e^{i\Omega}Q(\Omega), \tag{3.3}$$

here $Q(\Omega)$ is a real variable function.

By inserting this result into the earlier derived Eq. (3.2), we can decompose the result into its real and imaginary parts as shown below:

$$(-a\lambda_2 + \lambda_1)Q^3 + (a^3 - b)Q - 3a^3Q'' = 0. \tag{3.4}$$

$$-\frac{a(\lambda_2 + 2\lambda_3)}{9}Q^3 + \frac{9a^3 - 3b}{9}Q + -\frac{a^3}{3}Q'' = 0. \tag{3.5}$$

The following relations can be derived by merging Eq. (3.4) and Eq. (3.5)

$$\frac{(-a\lambda_2 + \lambda_1)}{-\frac{a(\lambda_2 + 2\lambda_3)}{9}} = \frac{(a^3 - b)}{\frac{9a^3 - 3b}{9}} = \frac{-3a^3}{-\frac{a^3}{3}}. \tag{3.6}$$

From Eq. (3.6), we obtain

$$a = -\frac{\lambda_1}{2\lambda_3}, b = \frac{a^3(-8a\lambda_2 + 2a\lambda_3 + 9\lambda_1)}{-2a\lambda_2 + 2a\lambda_3 + 3\lambda_1}. \tag{3.7}$$

Finally, Eq. (3.2) and Eq. (3.3) can be written as

$$\alpha_1 Q^3(\Omega) + \alpha_2 Q(\Omega) + \alpha_3 Q''(\Omega) = 0, \tag{3.8}$$

where $\alpha_1 = -\frac{a(\lambda_2 + 2\lambda_3)}{9}, \alpha_2 = \frac{9a^3 - 3b}{9}, \alpha_3 = -\frac{a^3}{3}$.

Using the balance method (homogeneous prinicple) between Q'' and Q^3 in Eq. (3.3), it is determined that $n = 1$. Consequently, the solution given in Eq. (2.5) reduces to the following simplified form:

$$U(\Omega) = \frac{\iota_0 + \iota_1 \phi(\Omega) + \frac{\varepsilon_1}{\phi(\Omega)}}{\kappa_0 + \kappa_1 \phi(\Omega) + \frac{\tau_1}{\phi(\Omega)}}. \tag{3.9}$$

Substituting into Eq. (3.9) and applying the form given in Eq. (2.5), we obtain a polynomial expression in $\phi(\Omega)$. By grouping the terms according to powers of $\phi(\Omega)$ and setting each coefficient to zero, we solve the resulting system using Maple and determine the following parameter values:

$$\iota_0 = -\frac{\kappa_0\left(\frac{\pm\lambda\iota_1\sqrt{-\alpha_2\alpha_1}}{\alpha_2} - 2\nu\kappa_0\right)\alpha_2}{\pm 2\nu\kappa_0\sqrt{-\alpha_2\alpha_1} + \lambda\alpha_1\iota_1},\ \kappa_0 = \kappa_0,\ \kappa_1 = \pm\frac{\iota_1\sqrt{-\alpha_2\alpha_1}}{\alpha_2},\ \tau_1 = 0,$$

where κ_0, ι_1 are random.

Substituting the obtained values of the parameters into the solution (3.9) and utilizing Eq. (3.3), we arrive at the following result:

$$U(\Omega) = \frac{\alpha_2\{\iota_1\kappa_0(2\nu\phi(\Omega) - \lambda)\sqrt{-\alpha_2\alpha_1} + \phi(\Omega)\lambda\iota_1^2\alpha_1 + 2\nu\alpha_2\kappa_0^2\}}{(2\sqrt{-\alpha_2\alpha_1}\nu\kappa_0 + \lambda\iota_1\alpha_1)(\sqrt{-\alpha_2\alpha_1}\iota_1\phi(\Omega) + \kappa_0\alpha_2)} e^{i\Omega}. \tag{3.10}$$

When $\lambda^2 - 4\mu\nu > 0$ and $\mu\nu \neq 0$ or $\lambda\nu \neq 0$, $\omega = \sqrt{\lambda^2 - 4\mu\nu}$, $\theta = \sqrt{-\alpha_2\alpha_1}$,

$$U_1(\Omega) = \frac{\alpha_2((2\theta\kappa_0\nu + \lambda\iota_1\alpha_1)\omega\iota_1 \tanh((\omega/2)\eta) + 4\iota_1\kappa_0\lambda\nu\theta + \lambda^2\iota_1^2\alpha_1 - 4\nu^2\alpha_2\kappa_0^2)}{(2\kappa_0\nu\theta + \lambda\iota_1\alpha_1)(\theta\omega\iota_1 \tanh((\omega/2)\eta) + \lambda\iota_1\theta - 2\kappa_0\alpha_2\nu)} e^{i\Omega}, \tag{3.11}$$

$$U_2(\Omega) = \frac{\alpha_2((2\theta\kappa_0\nu + \lambda\iota_1\alpha_1)\omega\iota_1 \coth((\omega/2)\eta) + 4\iota_1\kappa_0\lambda\nu\theta + \lambda^2\iota_1^2\alpha_1 - 4\nu^2\alpha_2\kappa_0^2)}{(2\kappa_0\nu\theta + \lambda\iota_1\alpha_1)(\theta\omega\iota_1 \coth((\omega/2)\eta) + \lambda\iota_1\theta - 2\kappa_0\alpha_2\nu)} e^{i\Omega}, \tag{3.12}$$

$$U_3(\Omega) = \frac{\alpha_2((\tanh(\omega\eta) + I\,\mathrm{sech}(\omega\eta))(2\theta\kappa_0\nu + \lambda\iota_1\alpha_1)\omega\iota_1 + 4\iota_1\kappa_0\lambda\nu\theta - 4\nu^2\alpha_2\kappa_0^2 + \lambda^2\iota_1^2\alpha_1)}{(2\kappa_0\nu\theta + \lambda\iota_1\alpha_1)\{(\tanh(\omega\eta) + I\,\mathrm{sech}(\omega\eta))\theta\omega\iota_1 + \lambda\iota_1\theta - 2\kappa_0\alpha_2\nu\}} e^{i\Omega}, \tag{3.13}$$

$$U_4(\Omega) = \frac{\alpha_2\left((\tanh(\omega\eta) - I\,\mathrm{sech}(\omega\eta))(2\theta\kappa_0\nu + \lambda\iota_1\alpha_1)\omega\iota_1 - 4\iota_1\kappa_0\lambda\nu\theta + 4\nu^2\alpha_2\kappa_0^2 - \lambda^2\iota_1^2\alpha_1\right)}{(2\kappa_0\nu\theta + \lambda\iota_1\alpha_1)\{(\tanh(\omega\eta) - I\,\mathrm{sech}(\omega\eta))\theta\omega\iota_1 - \lambda\iota_1\theta + 2\kappa_0\alpha_2\nu\}} e^{i\Omega}, \tag{3.14}$$

$$U_5(\Omega) = \frac{\alpha_2\left((\coth(\omega\eta) + \mathrm{csch}(\omega\eta))(2\theta\kappa_0\nu + \lambda\iota_1\alpha_1)\omega\iota_1 + 4\iota_1\kappa_0\lambda\nu\theta - 4\nu^2\alpha_2\kappa_0^2 + \lambda^2\iota_1^2\alpha_1\right)}{(2\kappa_0\nu\theta + \lambda\iota_1\alpha_1)\{(\coth(\omega\eta) + \mathrm{csch}(\omega\eta))\theta\omega\iota_1 + \lambda\iota_1\theta - 2\kappa_0\alpha_2\nu\}} e^{i\Omega}, \tag{3.15}$$

$$U_6(\Omega) = \frac{\alpha_2\left((\coth(\omega\eta) - \mathrm{csch}(\omega\eta))(2\theta\kappa_0\nu + \lambda\iota_1\alpha_1)\omega\iota_1 + 4\iota_1\kappa_0\lambda\nu\theta - 4\nu^2\alpha_2\kappa_0^2 + \lambda^2\iota_1^2\alpha_1\right)}{(2\kappa_0\nu\theta + \lambda\iota_1\alpha_1)\{(\coth(\omega\eta) - \mathrm{csch}(\omega\eta))\theta\omega\iota_1 + \lambda\iota_1\theta - 2\kappa_0\alpha_2\nu\}} e^{i\Omega}, \tag{3.16}$$

$$U_7(\Omega) = \frac{\alpha_2\begin{pmatrix}(\tanh((\omega/4)\eta) + \coth((\omega/4)\eta))(2\theta\kappa_0\nu + \lambda\iota_1\alpha_1)\omega\iota_1 + 8\iota_1\kappa_0\lambda\nu\theta \\ -8\nu^2\alpha_2\kappa_0^2 + 2\lambda^2\iota_1^2\alpha_1\end{pmatrix}}{(2\kappa_0\nu\theta + \lambda\iota_1\alpha_1)\{(\tanh((\omega/4)\eta) + \coth((\omega/4)\eta))\theta\omega\iota_1 + 2\lambda\iota_1\theta - 4\kappa_0\alpha_2\nu\}} e^{i\Omega}, \tag{3.17}$$

$$U_8(\Omega) = \frac{\alpha_2\begin{pmatrix}2\iota_1\kappa_0\theta\{-2\lambda(A\sinh(\omega\eta) + B) + (\omega C - A\omega\cosh(\omega\eta))\} + 4\nu^2\alpha_2\kappa_0^2(A\sinh(\omega\eta) + B) \\ +\lambda\iota_1^2\alpha_1\{-\lambda(A\sinh(\omega\eta) + B) + (\omega C - A\omega\cosh(\omega\eta))\}\end{pmatrix}}{(2\kappa_0\nu\theta + \lambda\iota_1\alpha_1)\{2\nu\kappa_0\alpha_2(A\sinh(\omega\eta) + B) + \iota_1\theta(-\lambda(A\sinh(\omega\eta) + B) + (\omega C - A\omega\cosh(\omega\eta)))\}} e^{i\Omega}, \tag{3.18}$$

$$U_9(\Omega) = \frac{\alpha_2\begin{pmatrix}2\iota_1\kappa_0\theta\{-2\lambda(A\sinh(\omega\eta) + B) + (-\omega C - A\omega\cosh(\eta\omega))\} + 4\nu^2\alpha_2\kappa_0^2(A\sinh(\omega\eta) + B) \\ +\lambda\iota_1^2\alpha_1\{-\lambda(A\sinh(\omega\eta) + B) + (-\omega C - A\omega\cosh(\omega\eta))\}\end{pmatrix}}{(2\kappa_0\nu\theta + \lambda\iota_1\alpha_1)\{2\nu\kappa_0\alpha_2(A\sinh(\omega\eta) + B) + \iota_1\theta(-\lambda(A\sinh(\omega\eta) + B) + (-\omega C - A\omega\cosh(\omega\eta)))\}} e^{i\Omega}, \tag{3.19}$$

$$U_{10}(\Omega) = \frac{\alpha_2\begin{pmatrix}2\iota_1\kappa_0\theta\{-2\lambda(A\sinh(\omega\eta) + B) - (\omega C + A\omega\cosh(\eta\,\omega))\} + 4\nu^2\alpha_2\kappa_0^2(A\sinh(\omega\eta) + B) \\ +\lambda\iota_1^2\alpha_1\{-\lambda(A\sinh(\omega\eta) + B) - (\omega C + A\omega\cosh(\omega\eta))\}\end{pmatrix}}{(2\kappa_0\nu\theta + \lambda\iota_1\alpha_1)\{2\nu\kappa_0\alpha_2(A\sinh(\omega\eta) + B) + \iota_1\theta(-\lambda(A\sinh(\omega\eta) + B) - (\omega C + A\omega\cosh(\omega\eta)))\}} e^{i\Omega}, \tag{3.20}$$

$$U_{11}(\Omega)=\frac{\alpha_2\begin{pmatrix}2\iota_1\kappa_0\theta\{-2\lambda(A\sinh(\omega\eta)+B)-(-\omega C+A\omega\cosh(\eta\,\omega))\}+4\nu^2\alpha_2\kappa_0^2(A\sinh(\omega\eta)+B)\\+\lambda\iota_1^2\alpha_1\{-\lambda(A\sinh(\omega\eta)+B)-(-\omega C+A\omega\cosh(\omega\eta))\}\end{pmatrix}}{(2\kappa_0\nu\theta+\lambda\iota_1\alpha_1)\{2\nu\kappa_0\alpha_2(A\sinh(\omega\eta)+B)+\iota_1\theta(-\lambda(A\sinh(\omega\eta)+B)-(-\omega C+A\omega\cosh(\omega\eta)))\}}e^{i\Omega}, \quad (3.21)$$

where A and B are two parameters with $B^2-A^2>0$ and $C=\sqrt{(A^2+B^2)}$.

$$U_{12}(\Omega)=\frac{\alpha_2\begin{pmatrix}-\sinh((\omega/2)\eta)\omega\kappa_0(\iota_1\lambda\theta-2\nu\alpha_2\kappa_0)+\\(-2\lambda\nu\alpha_2\kappa_0^2+\iota_1((\theta(4\mu\nu+\lambda^2)\kappa_0+2\mu\lambda\iota_1\alpha_1))\cosh((\omega/2)\eta)\end{pmatrix}}{(2\kappa_0\nu\theta+\lambda\iota_1\alpha_1)(\sinh((\omega/2)\eta)\omega\kappa_0\alpha_2+\cosh((\omega/2)\eta)(2\mu\iota_1\theta-\lambda\alpha_2\kappa_0))}e^{i\Omega}, \quad (3.22)$$

$$U_{13}(\Omega)=\frac{\alpha_2\begin{pmatrix}-\cosh((\omega/2)\eta)\omega\kappa_0(\iota_1\lambda\theta-2\nu\alpha_2\kappa_0)+\\(-2\lambda\nu\alpha_2\kappa_0^2+\iota_1((\theta(4\mu\nu+\lambda^2)\kappa_0+2\mu\lambda\iota_1\alpha_1))\sinh((\omega/2)\eta)\end{pmatrix}}{(2\kappa_0\nu\theta+\lambda\iota_1\alpha_1)(\cosh((\omega/2)\eta)\omega\kappa_0\alpha_2+\sinh((\omega/2)\eta)(2\mu\iota_1\theta-\lambda\alpha_2\kappa_0))}e^{i\Omega}, \quad (3.23)$$

$$U_{14}(\Omega)=-\frac{\alpha_2\begin{pmatrix}(-4\iota_1\theta(4\mu\nu+\lambda^2)\kappa_0-8\lambda(\mu\iota_1^2\alpha_1-\nu\alpha_2\kappa_0^2))\cosh(\omega\eta)\\+4\kappa_0(I+\sinh(\omega\eta))(\lambda\iota_1\theta-2\nu\kappa_0\alpha_2)\omega\end{pmatrix}}{4(2\kappa_0\nu\theta+\lambda\iota_1\alpha_1)((2\iota_1\mu\theta-\lambda\alpha_2\kappa_0)\cosh(\omega\eta)+\kappa_0(I+\sinh(\omega\eta))\omega\alpha_2)}e^{i\Omega}, \quad (3.24)$$

$$U_{15}(\Omega)=-\frac{\alpha_2\begin{pmatrix}(-4\iota_1\theta(4\mu\nu+\lambda^2)\kappa_0+8\lambda(\mu\iota_1^2\alpha_1-\nu\alpha_2\kappa_0^2))\cosh(\omega\eta)\\+4\kappa_0(I-\sinh(\omega\eta))(\lambda\iota_1\theta-2\nu\kappa_0\alpha_2)\omega\end{pmatrix}}{4(2\kappa_0\nu\theta+\lambda\iota_1\alpha_1)((-2\iota_1\mu\theta+\lambda\alpha_2\kappa_0)\cosh(\omega\eta)+\kappa_0(I-\sinh(\omega\eta))\omega\alpha_2)}e^{i\Omega}, \quad (3.25)$$

$$U_{16}(\Omega)=-\frac{\alpha_2\begin{pmatrix}\iota_1\kappa_0\theta\{4\nu\mu\sinh(\omega\eta)-\lambda(-\lambda\sinh(\omega\eta)+\omega\cosh(\omega\eta)+\omega))+\\2((\mu\sinh(\omega\eta)\lambda\iota_1^2\alpha_1)+\nu\alpha_2\kappa_0^2(-\lambda\sinh(\omega\eta)+\omega\cosh(\omega\eta)+\omega))\}\end{pmatrix}}{(2\kappa_0\nu\theta+\lambda\iota_1\alpha_1)((2\mu\iota_1\theta\sinh(\omega\eta))+\kappa_0\alpha_2(-\lambda\sinh(\omega\eta)+\omega\cosh(\omega\eta)+\omega))}e^{i\Omega}, \quad (3.26)$$

$$U_{17}(\Omega)=\frac{\alpha_2\begin{pmatrix}\iota_1\kappa_0\theta\{4\nu\mu\sinh(\omega\eta)-\lambda(-\lambda\sinh(\omega\eta)+\omega\cosh(\omega\eta)-\omega))+\\2((\mu\sinh(\omega\eta)\lambda\iota_1^2\alpha_1)+\nu\alpha_2\kappa_0^2(-\lambda\sinh(\omega\eta)+\omega\cosh(\omega\eta)-\omega))\}\end{pmatrix}}{(2\kappa_0\nu\theta+\lambda\iota_1\alpha_1)((2\mu\iota_1\theta\sinh(\omega\eta))+\kappa_0\alpha_2(-\lambda\sinh(\omega\eta)+\omega\cosh(\omega\eta)-\omega))}e^{i\Omega}, \quad (3.27)$$

$$U_{18}(\Omega)=\frac{\alpha_2\begin{pmatrix}(2\cosh((\omega/4)\eta)^2-1)\kappa_0(\theta\lambda\iota_1-2\nu\alpha_2\kappa_0)\omega-\\2(-2\lambda\nu\alpha_2\kappa_0^2+\iota_1(\kappa_0\theta(4\mu\nu+\lambda^2)+2\mu\lambda\iota_1\alpha_1))\\\sinh((\omega/4)\eta)\cosh((\omega/4)\eta)\end{pmatrix}}{\begin{matrix}(2\kappa_0\nu\theta+\lambda\iota_1\alpha_1)(\alpha_2(2\cosh((\omega/4)\eta)^2-1)\kappa_0\omega+4\sinh((\omega/4)\eta)\\(\iota_1\mu\theta-(\lambda\alpha_2\kappa_0/2))\cosh((\omega/4)\eta))\end{matrix}}e^{i\Omega}, \quad (3.28)$$

where, $\omega=\sqrt{\lambda^2-4\mu\nu}$, $\theta=\sqrt{-\alpha_2\alpha_1}$.

When $\lambda^2-4\mu\nu<0$ and $\lambda\mu\neq0$ or $\mu\nu\neq0$,

$$U_{19}(\Omega)=\frac{\alpha_2((2\theta\kappa_0\nu+\lambda\iota_1\alpha_1)\omega_1\iota_1\tan(\omega_1\eta/2)-4\iota_1\kappa_0\lambda\nu\theta+\lambda^2\iota_1^2\alpha_1-4\nu^2\alpha_2\kappa_0^2)}{(2\kappa_0\nu\theta+\lambda\iota_1\alpha_1)(\theta\omega_1\iota_1\tan(\omega_1\eta/2)-\lambda\iota_1\theta+2\kappa_0\alpha_2\nu)}e^{i\Omega}, \quad (3.29)$$

$$U_{20}(\Omega)=\frac{\alpha_2((2\theta\kappa_0\nu+\lambda\iota_1\alpha_1)\omega_1\iota_1\cot(\omega_1\eta/2)+4\iota_1\kappa_0\lambda\nu\theta+\lambda^2\iota_1^2\alpha_1-4\nu^2\alpha_2\kappa_0^2)}{(2\kappa_0\nu\theta+\lambda\iota_1\alpha_1)(\theta\omega_1\iota_1\cot(\omega_1\eta/2)+\lambda\iota_1\theta-2\kappa_0\alpha_2\nu)}e^{i\Omega}, \quad (3.30)$$

$$U_{21}(\Omega)=\frac{\alpha_2\left((\tanh(\omega_1\eta)-\sec(\omega_1\eta))(2\theta\kappa_0\nu+\lambda\iota_1\alpha_1)\omega_1\iota_1-4\iota_1\kappa_0\lambda\nu\theta+4\nu^2\alpha_2\kappa_0^2-\lambda^2\iota_1^2\alpha_1\right)}{(2\kappa_0\nu\theta+\lambda\iota_1\alpha_1)\{(\tan(\omega_1\eta)-\sec(\omega_1\eta))\theta\omega_1\iota_1-\lambda\iota_1\theta+2\kappa_0\alpha_2\nu\}}e^{i\Omega}, \quad (3.31)$$

$$U_{22}(\Omega)=\frac{\alpha_2\left((\tanh(\omega_1\eta)+\sec(\omega_1\eta))(2\theta\kappa_0\nu+\lambda\iota_1\alpha_1)\omega_1\iota_1-4\iota_1\kappa_0\lambda\nu\theta+4\nu^2\alpha_2\kappa_0^2-\lambda^2\iota_1^2\alpha_1\right)}{(2\kappa_0\nu\theta+\lambda\iota_1\alpha_1)\{(\tan(\omega_1\eta)+\sec(\omega_1\eta))\theta\omega_1\iota_1-\lambda\iota_1\theta+2\kappa_0\alpha_2\nu\}}e^{i\Omega}, \quad (3.32)$$

$$U_{23}(\Omega)=\frac{\alpha_2\left((\cot(\omega_1\eta)+\csc(\omega_1\eta))(2\theta\kappa_0\nu+\lambda\iota_1\alpha_1)\omega_1\iota_1+4\iota_1\kappa_0\lambda\nu\theta-4\nu^2\alpha_2\kappa_0^2+\lambda^2\iota_1^2\alpha_1\right)}{(2\kappa_0\nu\theta+\lambda\iota_1\alpha_1)\{(\cot(\omega_1\eta)+\csc(\omega_1\eta))\theta\omega_1\iota_1+\lambda\iota_1\theta-2\kappa_0\alpha_2\nu\}}e^{i\Omega}, \quad (3.33)$$

$$U_{24}(\Omega)=\frac{\alpha_2\left((\cot(\omega_1\eta)-\csc(\omega_1\eta))(2\theta\kappa_0\nu+\lambda\iota_1\alpha_1)\omega_1\iota_1+4\iota_1\kappa_0\lambda\nu\theta-4\nu^2\alpha_2\kappa_0^2+\lambda^2\iota_1^2\alpha_1\right)}{(2\kappa_0\nu\theta+\lambda\iota_1\alpha_1)\{(\cot(\omega_1\eta)-\csc(\omega_1\eta))\theta\omega_1\iota_1+\lambda\iota_1\theta-2\kappa_0\alpha_2\nu\}}e^{i\Omega}, \quad (3.34)$$

$$U_{25}(\Omega)=\frac{\alpha_2\left((\cot((\omega_1/4)\eta)-\tan((\omega_1/4)\eta))(2\theta\kappa_0\nu+\lambda\iota_1\alpha_1)\omega\iota_1+8\iota_1\kappa_0\lambda\nu\theta-8\nu^2\alpha_2\kappa_0^2+2\lambda^2\iota_1^2\alpha_1\right)}{(2\kappa_0\nu\theta+\lambda\iota_1\alpha_1)\{(\cot((\omega_1/4)\eta)-tan((\omega_1/4)\eta))\theta\omega\iota_1+2\lambda\iota_1\theta-4\kappa_0\alpha_2\nu\}}e^{i\Omega}, \quad (3.35)$$

$$U_{26}(\Omega)=\frac{\alpha_2\begin{pmatrix}2\iota_1\kappa_0\theta\{-2\lambda(A\sin(\omega_1\eta)+B)+(\omega_1C_1-A\omega_1\cos(\omega_1\eta))\}+4\nu^2\alpha_2\kappa_0^2(A\sin(\omega_1\eta)+B)\\+\lambda\iota_1^2\alpha_1\{-\lambda(A\sin(\omega_1\eta)+B)+(\omega_1C_1-A\omega\cos(\omega_1\eta))\}\end{pmatrix}}{(2\kappa_0\nu\theta+\lambda\iota_1\alpha_1)\{2\nu\kappa_0\alpha_2(A\sin(\omega_1\eta)+B)+\iota_1\theta(-\lambda(A\sin(\omega_1\eta)+B)+(\omega_1C_1-A\omega_1\cos(\omega_1\eta)))\}}e^{i\Omega}, \quad (3.36)$$

$$U_{27}(\Omega)=\frac{\alpha_2\begin{pmatrix}2\iota_1\kappa_0\theta\{-2\lambda(A\sin(\omega_1\eta)+B)+(-\omega_1C_1-A\omega_1\cos(\omega_1\eta))\}+4\nu^2\alpha_2\kappa_0^2(A\sin(\omega_1\eta)+B)\\+\lambda\iota_1^2\alpha_1\{-\lambda(A\sin(\omega_1\eta)+B)+(-\omega_1C_1-A\omega\cos(\omega_1\eta))\}\end{pmatrix}}{(2\kappa_0\nu\theta+\lambda\iota_1\alpha_1)\{2\nu\kappa_0\alpha_2(A\sin(\omega_1\eta)+B)+\iota_1\theta(-\lambda(A\sin(\omega_1\eta)+B)+(-\omega_1C_1-A\omega_1\cos(\omega_1\eta)))\}}e^{i\Omega}, \quad (3.37)$$

$$U_{28}(\Omega)=\frac{\alpha_2\begin{pmatrix}2\iota_1\kappa_0\theta\{-2\lambda(A\sin(\omega_1\eta)+B)-(\omega_1C_1+A\omega_1\cos(\omega_1\eta))\}+4\nu^2\alpha_2\kappa_0^2(A\sin(\omega_1\eta)+B)\\+\lambda\iota_1^2\alpha_1\{-\lambda(A\sin(\omega_1\eta)+B)-(\omega_1C_1+A\omega\cos(\omega_1\eta))\}\end{pmatrix}}{(2\kappa_0\nu\theta+\lambda\iota_1\alpha_1)\{2\nu\kappa_0\alpha_2(A\sin(\omega_1\eta)+B)+\iota_1\theta(-\lambda(A\sin(\omega_1\eta)+B)+(\omega_1C_1+A\omega_1\cos(\omega_1\eta)))\}}e^{i\Omega}, \quad (3.38)$$

$$U_{29}(\Omega)=\frac{\alpha_2\begin{pmatrix}2\iota_1\kappa_0\theta\{-2\lambda(A\sin(\omega_1\eta)+B)-(-\omega_1C_1+A\omega_1\cos(\omega_1\eta))\}+4\nu^2\alpha_2\kappa_0^2(A\sin(\omega_1\eta)+B)\\+\lambda\iota_1^2\alpha_1\{-\lambda(A\sin(\omega_1\eta)+B)-(-\omega_1C_1+A\omega\cos(\omega_1\eta))\}\end{pmatrix}}{(2\kappa_0\nu\theta+\lambda\iota_1\alpha_1)\{2\nu\kappa_0\alpha_2(A\sin(\omega_1\eta)+B)+\iota_1\theta(-\lambda(A\sin(\omega_1\eta)+B)-(-\omega_1C_1-A\omega_1\cos(\omega_1\eta)))\}}e^{i\Omega}, \quad (3.39)$$

where in the solutions (3.37), (3.38) and (3.39), A and B are quantities satisfy $A^2-B^2>0$, $C_1=\sqrt{(A^2-B^2)}$.

$$U_{30}(\Omega)=\frac{\alpha_2\begin{pmatrix}\sin((\omega_1/2)\eta)\omega_1\kappa_0(\iota_1\lambda\theta-2\nu\alpha_2\kappa_0)+\\(-2\lambda\nu\alpha_2\kappa_0^2+\iota_1((\theta(4\mu\nu+\lambda^2)\kappa_0+2\mu\lambda\iota_1\alpha_1))\cos((\omega_1/2)\eta)\end{pmatrix}}{(2\kappa_0\nu\theta+\lambda\iota_1\alpha_1)(-\sinh((\omega_1/2)\eta)\omega_1\kappa_0\alpha_2+\cos((\omega_1/2)\eta)(2\mu\iota_1\theta-\lambda\alpha_2\kappa_0))}e^{i\Omega}, \quad (3.40)$$

$$U_{31}(\Omega)=\frac{\alpha_2\begin{pmatrix}-\cos((\omega_1/2)\eta)\omega_1\kappa_0(\iota_1\lambda\theta-2\nu\alpha_2\kappa_0)+\\(-2\lambda\nu\alpha_2\kappa_0^2+\iota_1((\theta(4\mu\nu+\lambda^2)\kappa_0+2\mu\lambda\iota_1\alpha_1))\sin((\omega_1/2)\eta)\end{pmatrix}}{(2\kappa_0\nu\theta+\lambda\iota_1\alpha_1)(\cos((\omega_1/2)\eta)\omega_1\kappa_0\alpha_2+\sin((\omega_1/2)\eta)(2\mu\iota_1\theta-\lambda\alpha_2\kappa_0))}e^{i\Omega}, \quad (3.41)$$

$$U_{32}(\Omega)=\frac{\alpha_2\begin{pmatrix}(\iota_1\theta(4\mu\nu+\lambda^2)\kappa_0+2\lambda(\mu\iota_1^2\alpha_1-\nu\alpha_2\kappa_0^2))\cos(\omega_1\eta)\\+\omega_1\kappa_0(1+\sin(\omega_1\eta))(\lambda\iota_1\theta-2\nu\kappa_0\alpha_2)\end{pmatrix}}{(2\kappa_0\nu\theta+\lambda\iota_1\alpha_1)\left((2\iota_1\mu\theta-\lambda\alpha_2\kappa_0)\cos(\omega_1\eta)-\kappa_0(1+\sin(\omega_1\eta))\omega_1\alpha_2\right)}e^{i\Omega}, \quad (3.42)$$

$$U_{33}(\Omega)=\frac{\alpha_2\begin{pmatrix}(\iota_1\theta(4\mu\nu+\lambda^2)\kappa_0+2\lambda(\mu\iota_1^2\alpha_1-\nu\alpha_2\kappa_0^2))\cos(\omega_1\eta)\\+\omega_1\kappa_0(-1+\sin(\omega_1\eta))(\lambda\iota_1\theta-2\nu\kappa_0\alpha_2)\end{pmatrix}}{(2\kappa_0\nu\theta+\lambda\iota_1\alpha_1)\left((2\iota_1\mu\theta-\lambda\alpha_2\kappa_0)\cos(\omega_1\eta)-\kappa_0(-1+\sin(\omega_1\eta))\omega_1\alpha_2\right)}e^{i\Omega}, \quad (3.43)$$

$$U_{34}(\Omega)=\frac{\alpha_2\begin{pmatrix}(\iota_1\theta(4\mu\nu+\lambda^2)\kappa_0+2\lambda(\mu\iota_1^2\alpha_1-\nu\alpha_2\kappa_0^2))\sin(\omega_1\eta)\\-\omega_1\kappa_0(1+\cos(\omega_1\eta))(\lambda\iota_1\theta-2\nu\kappa_0\alpha_2)\end{pmatrix}}{(2\kappa_0\nu\theta+\lambda\iota_1\alpha_1)\left((2\iota_1\mu\theta-\lambda\alpha_2\kappa_0)\sin(\omega_1\eta)+\kappa_0(1+\cos(\omega_1\eta))\omega_1\alpha_2\right)}e^{i\Omega}, \quad (3.44)$$

$$U_{35}(\Omega)=\frac{\alpha_2\begin{pmatrix}(\iota_1\theta(4\mu\nu+\lambda^2)\kappa_0+2\lambda(\mu\iota_1^2\alpha_1-\nu\alpha_2\kappa_0^2))\sin(\omega_1\eta)\\-\omega_1\kappa_0(-1+\cos(\omega_1\eta))(\lambda\iota_1\theta-2\nu\kappa_0\alpha_2)\end{pmatrix}}{(2\kappa_0\nu\theta+\lambda\iota_1\alpha_1)\left((2\iota_1\mu\theta-\lambda\alpha_2\kappa_0)\sin(\omega_1\eta)+\kappa_0(-1+\cos(\omega_1\eta))\omega_1\alpha_2\right)}e^{i\Omega}, \quad (3.45)$$

$$U_{36}(\Omega)=\frac{\begin{matrix}(2(-(cos(\omega_1\eta/4)^2\kappa_0(\theta\lambda\iota_1-2\nu\alpha_2\kappa_0)\omega_1)+(\kappa_0\iota_1\theta(4\mu\nu+\lambda^2)+2(\mu\lambda\iota_1^2\alpha_1-\lambda\nu\alpha_2\kappa_0^2))\\\sin(\omega_1\eta/4)\cosh(\omega_1\eta/4)+\omega_1\kappa_0(\lambda\iota_1\theta-2\nu\kappa_0\alpha_2))\alpha_2)\end{matrix}}{\begin{matrix}((2\kappa_0\nu\theta+\lambda\iota_1\alpha_1)(2(\cosh(\omega_1\eta/4)^2\alpha_2\kappa_0\omega_1)+2\sin(\omega_1\eta/4)(\iota_1\mu\theta-\lambda\alpha_2\kappa_0)\\\cos(\omega_1\eta/4)-\omega_1\alpha_2\kappa_0))\end{matrix}}e^{i\Omega}, \quad (3.46)$$

where, $\omega_1=\sqrt{-\lambda^2+4\mu\nu}$, $\theta=\sqrt{-\alpha_2\alpha_1}$.

When $\mu=0$ and $\lambda\nu\neq 0$,

$$U_{37}(\Omega)=\frac{(\alpha_2\left(\kappa_0\iota_1\nu(-2\lambda f_1-\lambda)\theta+2\nu^2\alpha_2\kappa_0^2(f_1+\cosh(\lambda\eta)-\sinh(\lambda\eta))-f_1\lambda^2\iota_1^2\alpha_1\right)}{(2\kappa_0\nu\theta+\lambda\iota_1\alpha_1)(-\theta\lambda\iota_1f_1+\kappa_0\alpha_2\nu(f_1+\cosh(\lambda\eta)-\sinh(\lambda\eta)))}e^{i\Omega}, \quad (3.47)$$

$$U_{38}(\Omega)=\frac{\alpha_2\begin{pmatrix}\kappa_0\iota_1\theta(-(2\lambda(\cosh(\lambda\eta)+\sinh(\lambda\eta))-\lambda(f_1+\cosh(\lambda\eta)+\sinh(\lambda\eta))))\\+4\nu^2\alpha_2\kappa_0^2(f_1+\cosh(\lambda\eta)+\sinh(\lambda\eta))-\lambda^2(\cosh(\lambda\eta)+\sinh(\lambda\eta))\iota_1^2\alpha_1\end{pmatrix}}{(2\kappa_0\nu\theta+\lambda\iota_1\alpha_1)\{-\theta\lambda\iota_1(\cosh(\lambda\eta)+\sinh(\lambda\eta))+\kappa_0\alpha_2\nu(l_1+\cosh(\lambda\eta)+\sinh(\lambda\eta))\}}e^{i\Omega}, \quad (3.48)$$

where l_1 is a constant (random).

When $\nu \neq 0, \mu = \lambda = 0$,

$$U_{39}(\Omega) = \frac{\alpha_2(\iota_1\kappa_0(-2\nu-\lambda(\nu\eta+l_1))\theta+2(\nu\eta+l_1)\nu\alpha_2\kappa_0^2-\lambda\iota_1^2\alpha_1)}{(2\kappa_0\nu\theta+\lambda\iota_1\alpha_1)(-\theta\iota_1+\kappa_0\alpha_2(\nu\eta+l_1))} e^{i\Omega}, \tag{3.49}$$

where l_1 is a constant (random).

4. Results and Discussion

This section of the study provides a visual analysis of the derived solitons. Here, we emphasize the selection of suitable values for the parameters (free). The impact of fractional differentiation on soliton characteristics is examined through both three-dimensional and two-dimensional visualizations. The evolution of the solitons is depicted through 3D surfaces and 2D profiles. These graphical illustrations offer deeper understanding of the core physical processes involved. The 3D plots capture the soliton behavior over space and time and the 2D representations highlight how different values of the fractional-order derivative affect the soliton wave. All visual outputs have been generated using MATLAB.

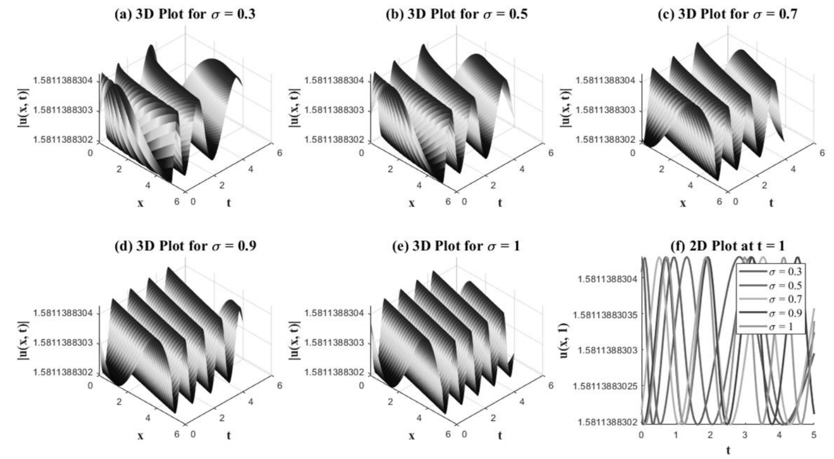

Fig.1: Shows the graphical visualization of the modulus plot of solution (3.27) with parameters, $\lambda_1 = 1, \sigma = 0.3,0.5,0.7,0.9,, \quad \lambda = 0.25, \mu = 1, \nu = .5, \iota_1 = 0.5, \kappa_0 = 0.5, \quad \lambda_2 = 0.2, \lambda_3 = 0.2$, over the domain $x \in [-6,6]$ and $t \in [-6,6]$.

Fig. 1(a-e) shows the modulus plot of solution (3.27), prepared by means of the constraint values $\lambda_1 = 1, \sigma = 0.3,0.5,0.7,0.9,, \quad \lambda = 0.25, \mu = 1, \nu = .5, \iota_1 = 0.5, \kappa_0 = 0.5, \ \lambda_2 = 0.2, \lambda_3 = 0.2$, over the domain $x \in [-6,6]$ and $t \in [-6,6]$., even though Fig.1(f) is demonstrated 2D prototypical in connotation with different values of σ. The illustrated wave represents the form of a periodic-type soliton. When we changes the values of the fractional parameterσ, the soliton changes into smoother, increasing the frequency, and shows the variation in phase. In the field of nonlinear optics, periodic solitons are employed to model light pulses. This property is particularly useful in the development of high-speed communication technologies. Similarly, in plasma physics, periodic soliton solutions are applied to describe wave structures like ion-acoustic and dust acoustic waves. This type of solitons provides valuable insight into the behavior of nonlinear waves in both laboratory and space plasma environments.

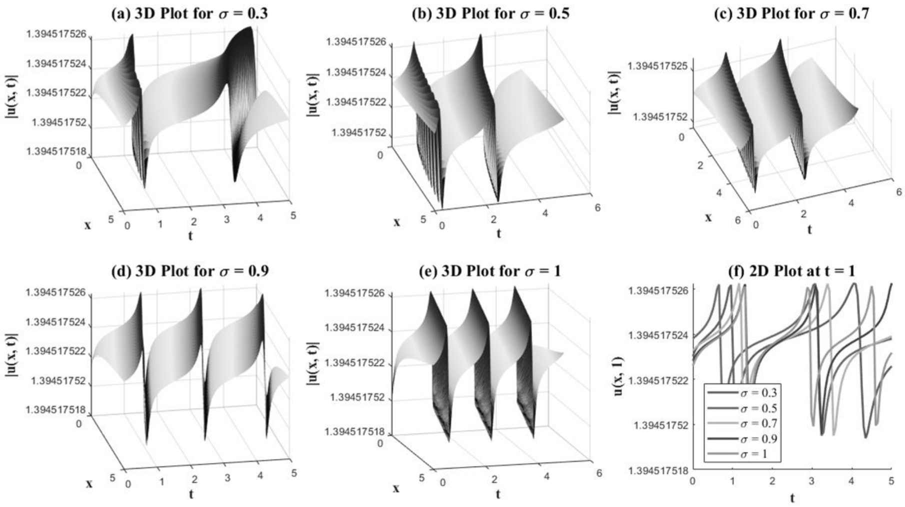

Fig.2: Shows the graphical visualization of the modulus plot of the (3.31) with parameters, $\lambda_1 = 1.79, \sigma = 0.3,0.5,0.7,0.9,1,$ $\lambda = 0.5, \mu = 0.1, \nu = 1.75, \iota_1 = 0.5, \kappa_0 = 0.75,$ $\lambda_2 = 0.4, \lambda_3 = 0.79,$, over the domain $x \in [-10,10]$ and $t \in [-10,10]$.

Fig. 2(a-e) shows the modulus plot of solution (3.31), prepared by means of the constraint values $\lambda_1 = 1.79, \sigma = 0.3,0.5,0.7,0.9,1,$ $\lambda = 0.5, \mu = 0.1, \nu = 1.75, \iota_1 = 0.5, \kappa_0 = 0.75,$ $\lambda_2 = 0.4, \lambda_3 = 0.79$, over the domain $x \in [-10,10]$ and $t \in [-10,10]$; even though Fig.2(f) is demonstrated 2D prototypical in association with different values of σ. The obtained wave shows the form of a quasi-periodic-type soliton. In optical fibers and photonic crystals, quasi-periodic solitons represent stable light pulses that preserve their shape by balancing dispersion with nonlinear effects. Similarly, in fluid systems, these solitons can describe wave patterns on the surface or at the interface of fluid layers.

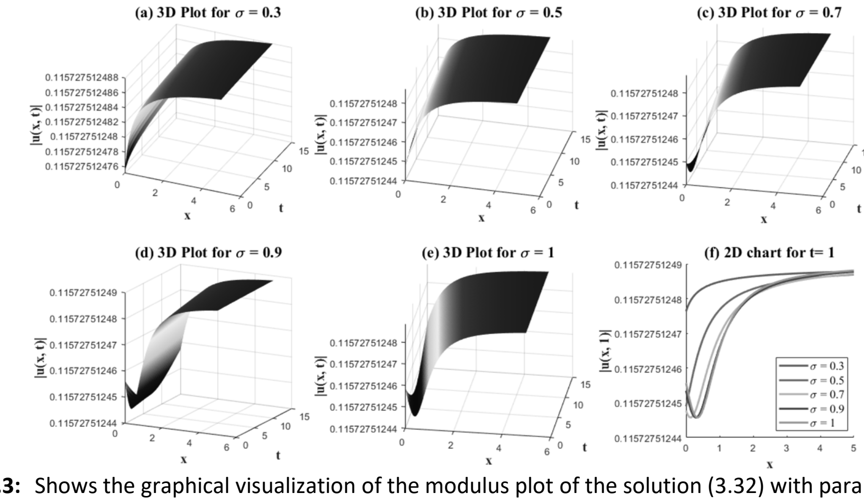

Fig.3: Shows the graphical visualization of the modulus plot of the solution (3.32) with parameters $\lambda_1 = 1, \sigma = 0.3,0.5,0.7,0.9,1,$ $\lambda = 2, \mu = 1, \nu = 2, \iota_1 = 0.5, \kappa_0 = 5,$ $\lambda_2 = 2.05, \lambda_3 = 3.45,$ over the domain $x \in [-5,5]$ and $t \in [-5,5]$.

Fig. 3(a-e) shows the modulus plot of solution (3.31), prepared by means of the constraint values $\lambda_1 = 1, \sigma = 0.3, 0.5, 0.7, 0.9, 1,$ $\lambda = 2, \mu = 1, \nu = 2, \iota_1 = 0.5, \kappa_0 = 5,$ $\lambda_2 = 2.05, \lambda_3 = 3.45,$ over the domain $x \in [-5,5]$ and $t \in [-5,5]$.; even though Fig.3(f) is demonstrated 2D prototypical in association with different values of σ. The consequential wave yields the form of an asymptotic soliton. In systems described by the GNLSE, asymptotic solitons illustrate how an initial wave packet gradually separates into individual, stable structures as it travels over long distances. They also play a crucial role in demonstrating the long-term stability of solitons and their predominance in the evolution of a wide range of initial waveforms.

5. Bifurcation analysis

Here, we discuss the bifurcation analysis of the prescribed model using dynamical system approach. Taking, $\frac{\alpha_2}{\alpha_3} = \rho_1, \frac{\alpha_1}{\alpha_3} = \rho_2$, then by assuming $X = Q$ and $Y = X'$, we hypothesize that the ODE delineated in Eq. (3.8) can be stated as:

$$\begin{cases} \frac{dX}{d\Omega} = Y \\ \frac{dY}{d\Omega} = -\rho_1 X - \rho_2 X^3 \end{cases}, \tag{5.1}$$

associated to the Hamiltonian

$$H(X,Y) = \frac{\rho_1}{2} X^2 + \frac{\rho_2}{4} X^4 + \frac{1}{2} Y^2. \tag{5.2}$$

For the system (6.1), the Jacobian matrix (JM) is noted as:

$$J(X,Y) = \begin{bmatrix} 0 & 1 \\ -\rho_1 - 3\rho_2 X^2 & 0 \end{bmatrix}.$$

In this framework, we present the recognized phase portrayals in the (X,Y)-plane in view of the cases below:

Case-I: When $\rho_1 > 0$ and $\rho_2 > 0$, there is one equilibrium point-(EP) of the system (6.1) at the origin $(0,0)$. At this EP the eigenvalues (EVs) corresponding to the JM are $\sqrt{-\rho_1}, -\sqrt{-\rho_1}$ viewing that the EP at the origin is a stable center portrayed in the Fig 4(a).

Case II: When $\rho_1 > 0$ and $\rho_2 < 0$, there are three distinct EPs of the system (6.1) namely $(0,0)$, $\left(\sqrt{-\frac{\rho_1}{\rho_2}}, 0\right)$ and $\left(-\sqrt{-\frac{\rho_1}{\rho_2}}, 0\right)$. The EVs of $J(0,0)$ are $\sqrt{-\rho_1}$, $-\sqrt{-\rho_1}$, showing that $(0,0)$ is a stable center. In a similar manner, the EVs of the other JM $J\left(\pm\sqrt{-\frac{\rho_1}{\rho_2}}, 0\right)$ are $\pm\sqrt{2\rho_1}$. Therefore, the EPs $\left(\pm\sqrt{-\frac{\rho_1}{\rho_2}}, 0\right)$ are unstable saddle points portrayed in Fig 4(b).

Case III: When $\rho_1 < 0$ and $\rho_2 > 0$, there are three distinct EPs of the system (6.1) namely $(0,0)$, $\left(\sqrt{-\frac{\rho_1}{\rho_2}}, 0\right)$ and $\left(-\sqrt{-\frac{\rho_1}{\rho_2}}, 0\right)$. The EVs of $J(0,0)$ are $\sqrt{-\rho_1}$, $-\sqrt{-\rho_1}$, showing that $(0,0)$ is a stable center. In a similar manner, the EVs of the other JM $J\left(\pm\sqrt{-\frac{\rho_1}{\rho_2}}, 0\right)$ are $\pm\sqrt{2\rho_1}$. Therefore, the EPs $\left(\pm\sqrt{-\frac{\rho_1}{\rho_2}}, 0\right)$ are unstable saddle points portrayed in Fig 4(c).

Case IV: When $\rho_1 < 0$ and $\rho_2 < 0$, there is only one equilibrium point of the system (6.1) at the origin $(0, 0)$. The EVs of $J(0,0)$ are $\sqrt{-\rho_1}$, $-\sqrt{-\rho_1}$, displaying that the EP origin is a stable center portrayed in Fig 4(d).

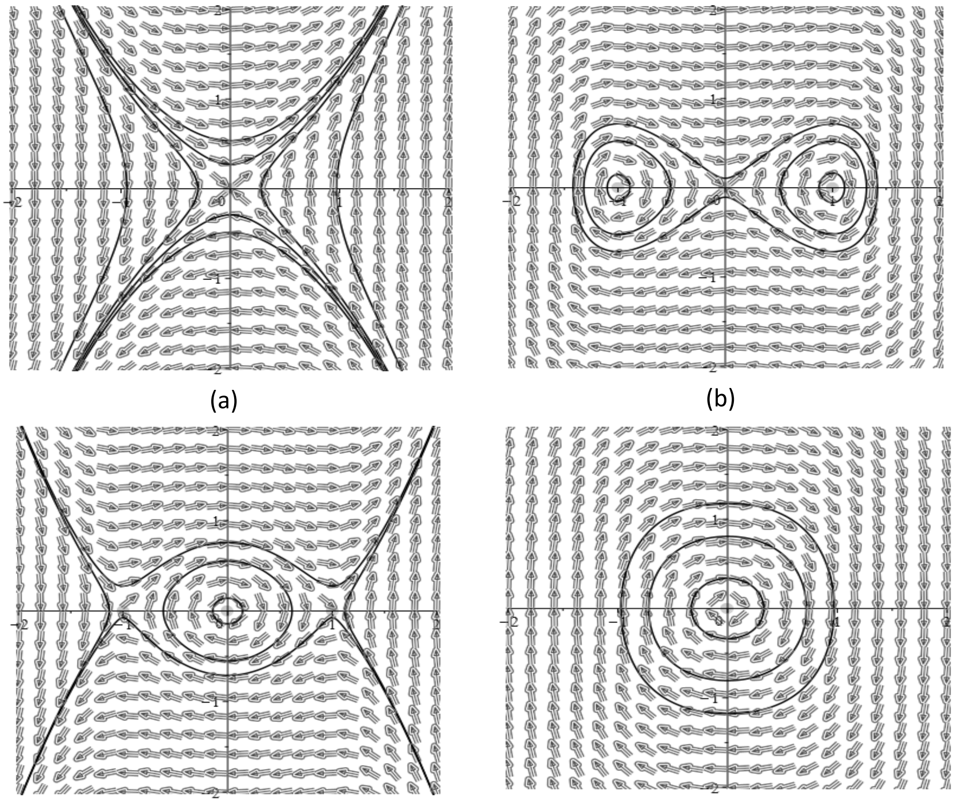

(a) (b) (c) (d)

Fig. 4: shows phase depictions for the system (6.1) with
(a) $\alpha_1 = 1, a_3 = 1, a_1 = -1, \alpha_2 = 1, a_4 = 2, \alpha_3 = 1, a_5 = -3/2, u = 1, k = -2$;
(b) $\alpha_1 = 1, a_1 = 1, a_3 = -1, \alpha_2 = -1, a_4 = 2, \alpha_3 = -1, a_5 = -\frac{3}{2}, k = 2, u = 1$;
(c) $\alpha_1 = 1, a_1 = -1, a_3 = -1, \alpha_2 = 1, a_4 = -2, \alpha_3 = -1, a_5 = \frac{3}{2}, u = 1, k = -2$;
(d) $\alpha_1 = 1, a_3 = -1, a_1 = -1, \alpha_2 = 1, a_4 = 2, \alpha_3 = -1, a_5 = -\frac{3}{2}, k = -2, u = 1$.

6. Chaotic and Sensitivity analysis

The chaotic behavior of nonlinear evolution equations reflects the complexity, sensitivity, and unpredictability of their solutions under certain conditions. Some slight changes in initial or boundary values can lead to drastically different results in chaotic dynamics. We examined the perturbation term $\omega\cos(\mu t)$, where ω represents the amplitude and μ denotes the frequency to investigate the chaotic characteristics of the system shown in equation (5.1). This allowed us to gain insight into the dynamic characteristics of the system:

$$\begin{cases} \dfrac{dX}{d\Omega} = Y \\ \dfrac{dY}{d\Omega} = -\rho_1 X - \rho_2 X^3 + \omega\cos(\mu t) \end{cases}$$
(6.1)

We examine how variations in the disturbance amplitude and frequency influence the behavior of system (6.1). We assign specific values to the parameters and initial conditions as shown in Fig. 5 and in Fig. 6. To illustrate the system's chaotic behavior graphically, we use the following parameter values and initial conditions: in Fig. 5, the values are set as $a = 1, b = -2, c = 4, w = 1, w_1 = 4, w_2 = 1$, $\omega = 0.017, \mu = 2\pi$, with initial conditions X(0)= 0.5 and Y(0)=0; in Fig.6, $a = 1, b = 4, c = 4, w = 1, w_1 = 4, w_2 = 1, \omega = 1$, and $\mu = \pi/4$; in the points, $X(0) = 0$ and $Y\ (0) = 0.1$.

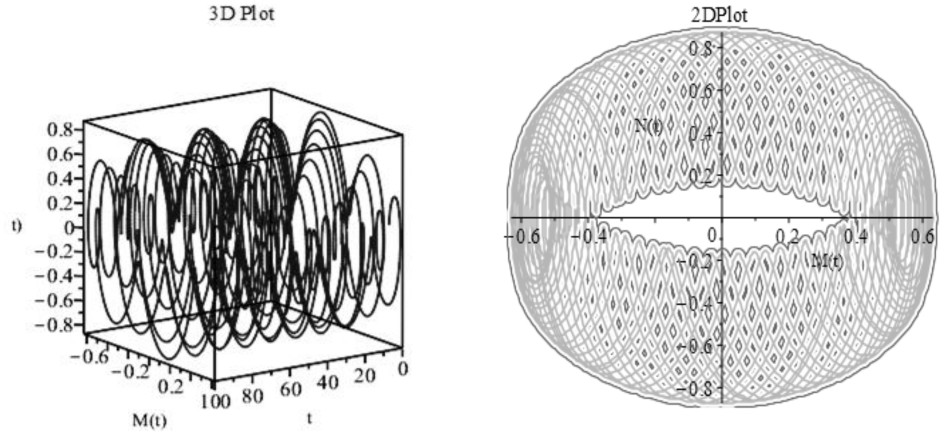

Fig .5: Chaotic structures of values with ω and the dynamic construction that has been labeled for $a = 1, b = -2, c = 4, w = 1, w_1 = 4, w_2 = 1$, $\omega = 0.017, \mu = 2\pi$.

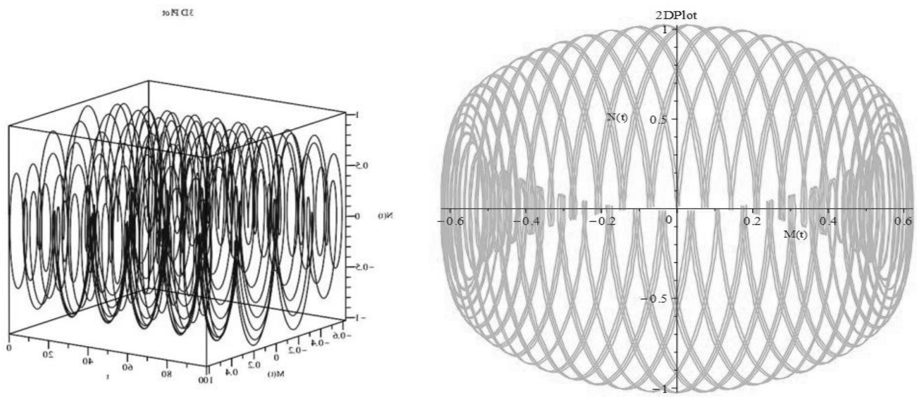

Fig. 6: Chaotic structures of values with μ and the dynamic construction that has been designated for $a = 1, b = 4, c = 4, w = 1, w_1 = 4, w_2 = 1, \omega = 1$, and $\mu = \pi/4$.

Here we have analyzed the sensitivity of the system described by equation (6.1). This analysis is conducted using a specified set of parameter values: $a = 1, b = -2, c = 4, w = 1, w_1 = 1, w_2 = 4$; and the conditions for the system (6.1) are: $X(0) = 0.3$ and $Y(0) = 0; X(0) = 0$ and $Y(0) = 0.1$.

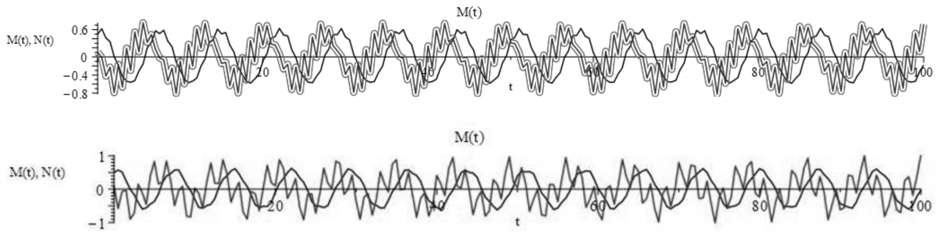

Fig. 7: A sensitivity test for (6.1) is demonstrated using a specified set of parameter values: $a = 1, b = -2, c = 4, w = 1, w_1 = 1, w_2 = 4$; where $X = M$ and $Y = N$.

7. Conclusion

In this study, we have obtained thirty nine soliton solutions of the space-time fractional GNLSE using the EREA. We have derived a variety of exact solutions like rational, trigonometric, and hyperbolic forms. We have shown different wave behaviors, such as periodic structures and localized solitons with graphical representations against the solutions. Furthermore, in bifurcation analysis, stable center, unstable saddle points corresponding to the equilibrium points $(0,0)$ and $\left(\pm\sqrt{-\frac{\rho_1}{\rho_2}}, 0\right)$ have been studied with visualization. Moreover, chaotic analysis, and sensitivity with initial conditions $X(0) = 0.3$ and $Y(0) = 0; X(0) = 0$ and $Y(0) = 0.1$ have been studied in this work. We hope that the outcomes of this study will contribute to nonlinear wave dynamics in complex dispersive media. A future research can be studied by examining the GNLSE using broader forms of fractional derivatives beyond the Beta derivative.

References

Ahmad, S., Salman, Ullah, A., Ahmad, S. & Akgül, A. (2023). Bright, dark and hybrid multistrip optical soliton solutions of a non-linear Schrödinger equation using modified extended tanh technique with new Riccati solutions, *Optical and Quantum Electronics*, 55:236.

Amin, M. A., Islam, M. N. & Akbar, M. A. (2025). Abundant closed-form solitary solutions of a nonlinear neurobiological model for analyzing numerous signal transmission behaviors through the neuron using recent scheme, *Partial Differ. Equ Appl Math.,* 13, 101051.

Amin, M. A., Akbar, M. A., Khan, M. A. & Sagib, M. (2025). Soliton solutions, bifurcations, and sensitivity analysis to the higher-order nonlinear fractional Schrödinger equation in optical fibers. *Partial Differ. Equ Appl Math.,* 13, 101057.

Arnous, A. Seadawy, A. Alqahtani, R. & Biswas, A. (2017). Optical solitons with complex Ginzburg-Landau equation by modified simple equation method. *Optik.,* 144, 475–480.

Atangana, A. (2016). Derivative with a New Parameter: Theory, Methods and Applications. *Academic Press, London, UK.*

Bekir, A. & Unsal, O. (2012). Analytic treatment of nonlinear evolution equations using first integral method. *Pram. J. Phys.,* 79(1), 3–17.

Bekir, A. & Boz, A. (2008). Exact solutions for nonlinear evolution equations using exp-function method. *Phys. Lett. A.,* 372(10), 1619–1625.

Caputo, M. (1967). Linear models of dissipation whose Q is almost frequency independent. Part II, *Geophys. J. Int.,* 13(5), 529-539.

Grünwald, A. (1867). Über "begrenzte Derivationen" und deren Anwendung. *Zeitschrift für Mathematik und Physik.,* 12, 441–480.

Inc, M. (2008). Application of homotopy analysis method for fin efficiency of convective straight fins with temperature-dependent thermal conductivity. *Math. Comput. Simu.,* 79(2), 189–200.

Jumarie, G. (2006) Modified Riemann-Lioville derivative and fractional Taylor series of non-differentiable functions further results, *Comput. Math. Appl*., 51(9-10), 367-376.

Kaplan, M., Bekir, A. & Bulut, A. (2016). Analytical solutions with the improved (G'/G)-expansion method for nonlinear evolution equations. *J. Phys*., 766: 012033.

Kawser M A et al. (2024). Temporal wave dynamics, phase portrait and qualitative analysis of the time-dependent (2+1)-dimensional Zakharov-Kuznetsov equation. *Phys. Scr.,* 99, 095266.

Khalil, R., Horani, A. M., Yousef, A. & Sababheh, M. (2014). A new definition of fractional derivative*. J. Comput. Appl. Math.,* 264: 65-70.

Khan et al. (2023). Dynamical properties and new optical soliton solutions of a generalized nonlinear Schrödinger equation, *Eur. Phys. J. Plus*, 138:1059

Kilic, B. & Inc, M. (2016). Soliton solutions for the Kundu-Eckhaus equation with the aid of unified algebraic and auxiliary equation expansion methods. *J. Elect. Wav. Appl*., 30(7), 871–879.

Letnikov, A. V. (1968). Theory of Differentiation of Arbitrary Order, *Matematicheskii Sbornik*, 3 (1), 1–68.

Liouville, J. (1832). Mémoire sur quelques questions de géométrie et de mécanique, et sur un nouveau genre de calcul pour résoudre ces questions, *J. de l'École Polytechnique*, 13, 1–69.

Liu, X.Z., Yu, J. & Lou, Z. M. (2018). New interaction solutions from residual symmetry reduction and consistent Riccati expansion of the (2+1)-dimensional Boussinesq equation. *Nonlinear Dyn*., 92(4), 1469–1479.

Lu, D., Seadawy, A.R., Wang, J., Arshad, M. & Farooq, U. (2019). Soliton solutions of the generalised third-order nonlinear Schrödinger equation by two mathematical methods and their stability. *Pramana,* 93, 1–9.

Miah, S. S., Akbar, M. A. & Khan, K. (2025a). Solitary wave solutions with stability, bifurcation, sensitivity and chaotic analysis of the (3+1)-dimensional Yu-Toda-Sasa-Fukuyama equation using beta derivative, *Partial Differ. Equ Appl Math*., 14, 101192.

Miah, S. S., Akbar, M. A. & Khan, K. (2025b). Solitary wave solutions and stability analysis of the fractional Sawada-Kotera equation using the extended modified auxiliary equation mapping method, *Journal of Umm Al-Qura University of Applied Sciences* (in press) https://doi.org/10.1007/s43994-025-00230-9

Tripathy, A. & Sahoo, S. (2023). Abundant explicit and exact solutions for the space-time fractional Vakhnenko-Parkes model in the relaxing medium with stability analysis. *Int. J. Mod. Phy.*; B 37(12), 2350286.

Wang, L. Y. & Gao, B. (2023). Exact solutions to the fractional complex Ginzburg-Landau equation ith time-dependent coefficients under quadratic-cubic and power law nonlinearities. *Nonlinear Dyn.*, 111, 4709–4722.

Zhu, S. (2008). The generalizing Riccati equation mapping method in non-linear evolution equation: Application to (2+1)-dimensional Boiti-Leon-Pempinelle equation. *Chaos, Solitons and Fractals*, 37(5), 1335-1342.